Electronic Supplementary Material (ESI) for Dalton Transactions.

Ferromagnetic Coupling in d^1-d^3 Linear Oxido-Bridged Heterometallic Complexes： Ground-State Models of Metal-to-Metal Charge Transfer Excited States

Tao Huang, Xinyuan Wu, Xiao Song, Hao Xu, Tatyana I. Smirnova, Walter W. Weare,* Roger D. Sommer

Department of Chemistry, North Carolina State University, Campus Box 8204,
Raleigh, NC, 27695-8204, United States of America.

*wwweare@ncsu.edu

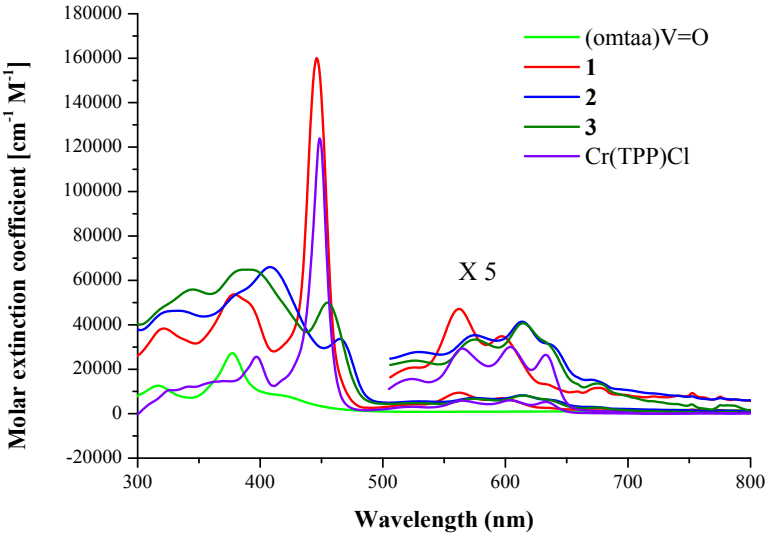

Figure S1. A) Molar absorptivity of the (omtaa)V═O, Cr(TPP)Cl, bimetallic **1** and trimetallic **2-3** in dichloromethane.

Details of electronic absorption spectra

The electronic absorption spectra of **1-3** are depicted in Figure S1 and summarized in Table S1. As can be seen in Figure S1, the change of the absorption spectrum of **1** is not significant when compared to its precursors. The (omtaa)V═O based absorption has a small red shift from 316 nm to 321 nm and the porphyrin based Soret band and Q bands remain similar to the Cr(III) porphyrin precursor.[1] The small differences in electronic absorption spectra is in contrast to previous examples of bimetallic Ti═O→Cr.[2] We believe the (omtaa)V═O in this bimetallic species can dissociate in solution at room temperature since the V═O→Cr is relative weakly bonded. Contrary to the small change in bimetallic species, the Soret band in trimetallic species is red shifted to 464 nm and the intensity dramatically decreases. The (omtaa)V═O based absorption at 420 nm is blue shifted to 408 nm and gains intensity. This intensity borrowing suggests a configuration interaction between these two chromophores. Detailed study of this unusual configuration interaction is still in progress. By comparing the electronic absorption spectrum of **2-3** with the precursor molecules and bimetallic species **1**, we conclude the trimetallic species remains stable in solution otherwise these significant differences in electronic absorption spectrum would not be observed.

Solid state ATR-FTIR spectra of **1-3** are depicted in Figure S6-8 and summarized Table S1. The V═O stretch is red shifted by 40~60 cm^{-1} when coordinated to chromium, which is in agreement with Goedken and coworkers.[3] The lower energy $\nu_{V=O}$ in **2** indicates that a stronger bonding interaction occurs in V═O→Cr than in the V═O→BPh_3 observed by Goedken.[4] As shown in Table S1, the bimetallic species **1** has $\nu_{V=O}$ at 933 cm^{-1} while trimetallic species **2** has $\nu_{V=O}$ frequency at 912 cm^{-1}. This shows a stronger interaction in the trimetallic species than the bimetallic species which is presumably due to different electronic properties of axial ligands as proposed in our previous study.[2] In trimetallic species, the (omtaa)V═O is believed to stabilize a second (omtaa)V═O which is *trans* to itself *via* a push-pull mechanism.[5-7] This observation is also consistent with the suggested instability of **1** in solution as observed using EAS.

X-ray Crystallography

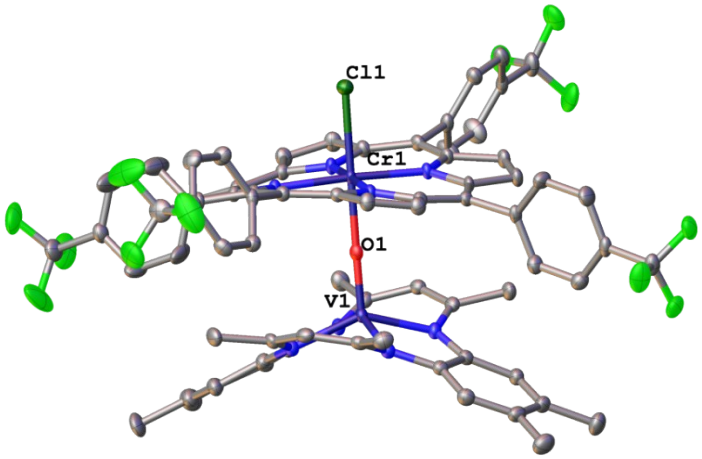

Figure S2. X-ray crystal structure of **1**. Thermal ellipsoids are drawn at 50% probability. Hydrogen atoms and solvent molecules are omitted for clarity.

A dark black block-like specimen of $C_{80}H_{66}Cl_{13}CrF_{12}N_8OV$, approximate dimensions 0.568 mm × 0.391 mm × 0.274 mm, was used for the X-ray crystallographic analysis. The X-ray intensity data were measured.

A total of 1097 frames were collected. The total exposure time was 21.53 hours. The frames were integrated with the Bruker SAINT software package using a narrow-frame algorithm. The integration of the data using a orthorhombic unit cell yielded a total of 102867 reflections to a maximum θ angle of 26.373° (0.80 Å resolution), of which 18323 were independent (average redundancy 5.61, completeness = 100.0 %, Rint = 4.28%, Rsig = 3.87%) and 13275 (72.45%) were greater than $2\sigma(F^2)$. The final cell constants of a = 13.1820(5) Å, b = 13.6961(6) Å, c = 27.0875(11) Å, volume = 4485.3(3) $Å^3$, are based upon the refinement of the XYZ-centroids of 9681 reflections above 20 σ(I) with 4.674° < 2θ < 52.904°. Data were corrected for absorption effects using the multi-scan method (SADABS). The ratio of minimum to maximum apparent transmission was 0.8347.

The structure was solved and refined using the Bruker SHELXTL Software Package, using the space group P-1, with Z = 2 for the formula unit, $C_{80}H_{66}Cl_{13}CrF_{12}N_8OV$. The final anisotropic full-matrix least-squares refinement on F_2 with 1092 variables converged at R_1 = 5.56 %, for the observed data and wR_2 = 16.55 % for all data. The goodness-of-fit was 1.044. The largest peak in the final difference electron density synthesis was 0.958 $e^-/Å^3$ and the largest hole was -1.005 $e^-/Å^3$ with an RMS deviation of 0.094 $e^-/Å^3$. On the basis of the final model, the calculated density was 1.442 g/cm^3 and F(000), 1972.0 e^-.

Disorders of dichloromethane solvent molecules were identified. The following chlorine atoms have partially occupancy Cl(1S): 0.36, Cl(2S): 0.64, Cl(3S): 0.64, Cl(4S): 0.36, Cl(5S): 0.659, Cl(6S): 0.314, Cl(9S): 0.41, Cl(10S): 0.59, respectively.

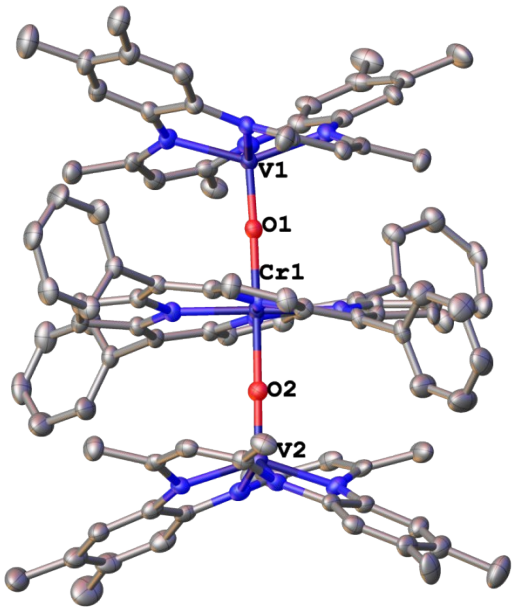

Figure S3. X-ray crystal structure of **2**. Thermal ellipsoids are drawn at 50% probability. Hydrogen atoms, SbF_6 anion and solvent molecules are omitted for clarity.

A metallic dark black block-like specimen of $C_{100}H_{96}Cl_8CrF_6N_{12}O_2SbV_2$, approximate dimensions 0.716 mm × 0.598 mm × 0.296 mm, was used for the X-ray crystallographic analysis. The X-ray intensity data were measured.

A total of 465 frames were collected. The total exposure time was 21.76 hours. The frames were integrated with the Bruker SAINT software package using a narrow-frame algorithm. The integration of the data using a orthorhombic unit cell yielded a total of 108776 reflections to a maximum θ angle of 25.680° (0.82 Å resolution), of which 18697 were independent (average redundancy 5.82, completeness = 99.8 %, Rint = 8.37%, Rsig = 4.66%) and 14133 (75.59%) were greater than $2\sigma(F^2)$. The final cell constants of a = 21.3129(7) Å, b = 22.2548(7) Å, c = 24.0941(9) Å, volume = 9869.3(6) $Å^3$, are based upon the refinement of the XYZ-centroids of 9996 reflections above 20 σ(I) with 4.716° < 2θ < 51.510°. Data were corrected for absorption effects using the multi-scan method (SADABS). The ratio of minimum to maximum apparent transmission was 0.7444.

The structure was solved and refined using the Bruker SHELXTL Software Package, using the space group $P2_1/c$, with Z = 4 for the formula unit, $C_{100}H_{96}Cl_8CrF_6N_{12}O_2SbV_2$. The final anisotropic full-matrix least-squares refinement on F_2 with 1251 variables converged at R_1 = 8.26 %, for the observed data and wR_2 =22.82 % for all data. The goodness-of-fit was 1.081. The largest peak in the final difference electron density synthesis was 1.193 e-/$Å^3$ and the largest hole was -1.599 $e^-/Å^3$ with an RMS deviation of 0.067 $e^-/Å^3$. On the basis of the final model, the calculated density was 1.461 g/cm^3 and F(000), 4427.9 e^-.

The Cl(6B) and Cl(6A) in one of the dichloromethane solvent molecule have partially occupancy of 0.3333 and 0.6667 respectively. PLAT019 (B level) alert was noticed by (IUCr) checkCIF. This is due to the relatively fast desolvation of this crystal that results in missing of reflections at lower resolution.

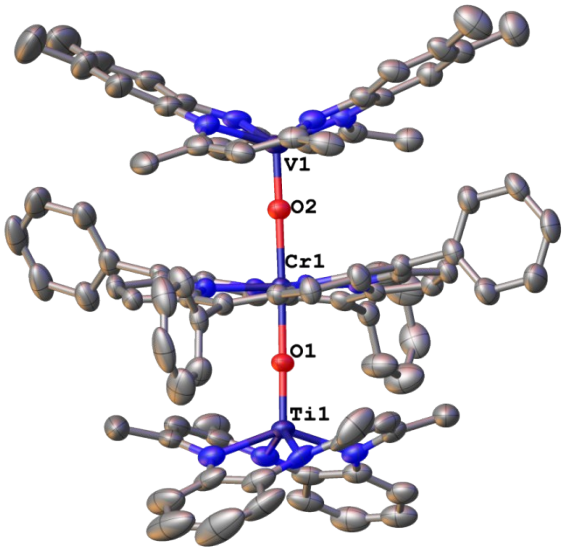

Figure S4. X-ray crystal structure of **3**. Thermal ellipsoids are drawn at 50% probability. Hydrogen atoms, SbF_6 anion and solvent molecules are omitted for clarity.

A metallic dark black plate-like specimen of $C_{92}H_{80}CrF_6N_{12}O_2SbTiV$, approximate dimensions 0.506 mm × 0.465 mm × 0.120 mm, was used for the X-ray crystallographic analysis. The X-ray intensity data were measured.

A total of 2337 frames were collected. The total exposure time was 42.80 hours. The frames were integrated with the Bruker SAINT software package using a narrow-frame algorithm. The integration of the data using a orthorhombic unit cell yielded a total of 203167 reflections to a maximum θ angle of 25.027° (0.84 Å resolution), of which 16810 were independent (average redundancy 12.28, completeness = 100.0 %, Rint = 4.09%, Rsig = 2.29%) and 12900 (76.74%) were greater than $2\sigma(F^2)$. The final cell constants of a = 18.4365(8) Å, b = 22.6229(10) Å, c = 24.1293(10) Å, volume = 9523.6(5) $Å^3$, are based upon the refinement of the XYZ-centroids of 9054 reflections above 20 σ(I) with 4.876° < 2θ < 50.568°. Data were corrected for absorption effects using the multi-scan method (SADABS). The ratio of minimum to maximum apparent transmission was 0.8833.

The structure was solved and refined using the Bruker SHELXTL Software Package, using the space group $P2_1/C$, with Z = 4 for the formula unit, $C_{92}H_{80}CrF_6N_{12}O_2SbTiV$. The final anisotropic full-matrix least-squares refinement on F_2 with 1109 variables converged at R_1 = 7.74 %, for the observed data and wR_2 = 21.22 % for all data. The goodness-of-fit was 1.150. The largest peak in the final difference electron density synthesis was 0.820 e-/$Å^3$ and the largest hole was -1.006 e-/$Å^3$ with an RMS deviation of 0.090 $e^-/Å^3$. On the basis of the final model, the calculated density was 1.474 g/cm^3 and F(000), 3624.0 e^-.

The SbF_6^- anion is found to be disordered in two orientations. They have partially occupancy of 0.3333 and 0,6667 respectively. PLAT019 (B level) alert was noticed by (IUCr) checkCIF. This is due to the quick desolvation of this crystal that results in missing of reflections at lower resolution. PLAT250 (B level) alert was noticed as well. No systematic errors in the data or errors in the model were found.

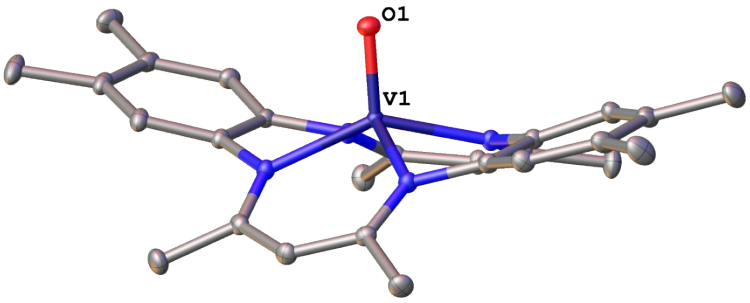

Figure S5. X-ray crystal structure of (omtaa)V═O. Thermal ellipsoids are drawn at 50% probability. Hydrogen atoms and solvent molecules are omitted for clarity.

A metallic dark black plate-like specimen of $C_{27}H_{32}Cl2N_4OV$, approximate dimensions 0.575 mm × 0.320 mm × 0.212 mm, was used for the X-ray crystallographic analysis. The X-ray intensity data were measured.

A total of 2547 frames were collected. The total exposure time was 18.43 hours. The frames were integrated with the Bruker SAINT software package using a narrow-frame algorithm. The integration of the data using a orthorhombic unit cell yielded a total of 43863 reflections to a maximum θ angle of 32.577° (0.66 Å resolution), of which 9191 were independent (average redundancy 4.77, completeness = 100.0 %, Rint = 1.47%, Rsig = 2.05%) and 8578 (93.33%) were greater than $2\sigma(F^2)$. The final cell constants of a = 8.5779(7) Å, b = 12.0788(10) Å, c = 12.8219(11) Å, volume = 1263.52(18) $Å^3$, are based upon the refinement of the XYZ-centroids of 9734 reflections above 20 σ(I) with 4.908° < 2θ < 78.398°. Data were corrected for absorption effects using the multi-scan method (SADABS). The ratio of minimum to maximum apparent transmission was 0.8669.

The structure was solved and refined using the Bruker SHELXTL Software Package, using the space group P-1, with Z = 4 for the formula unit, $C_{27}H_{32}Cl2N_4OV$. The final anisotropic full-matrix least-squares refinement on F_2 with 343 variables converged at R_1 = 3.30 %, for the observed data and wR_2 = 9.81 % for all data. The goodness-of-fit was 1.057. The largest peak in the final difference electron density synthesis was 0.583 e-/$Å^3$ and the largest hole was -0.813 e-/$Å^3$ with an RMS deviation of 0.072 $e^-/Å^3$. On the basis of the final model, the calculated density was 1.447 g/cm^3 and F(000), 574.0 e^-.

Electronic absorption and solid state ATR-FTIR spectra of **1**-**3**

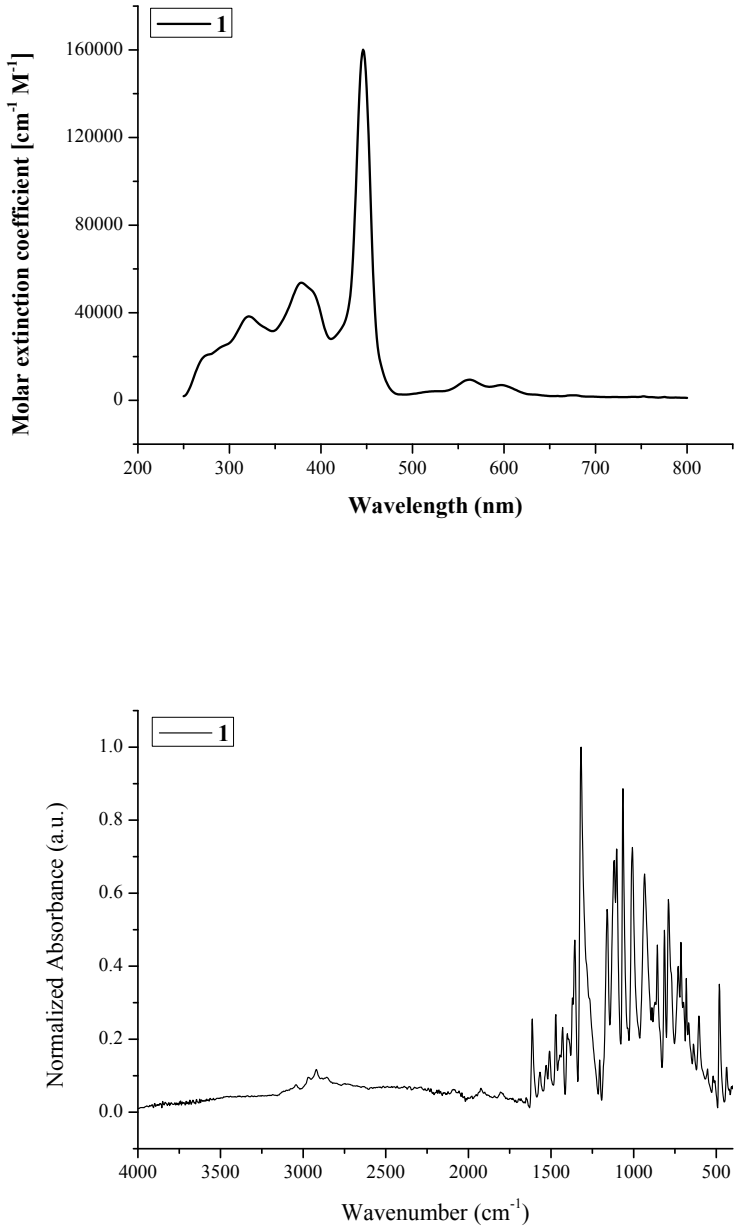

Figure S6. Molar absorptivity (in dichloromethane) and solid state ATR-FTIR spectra of **1**.

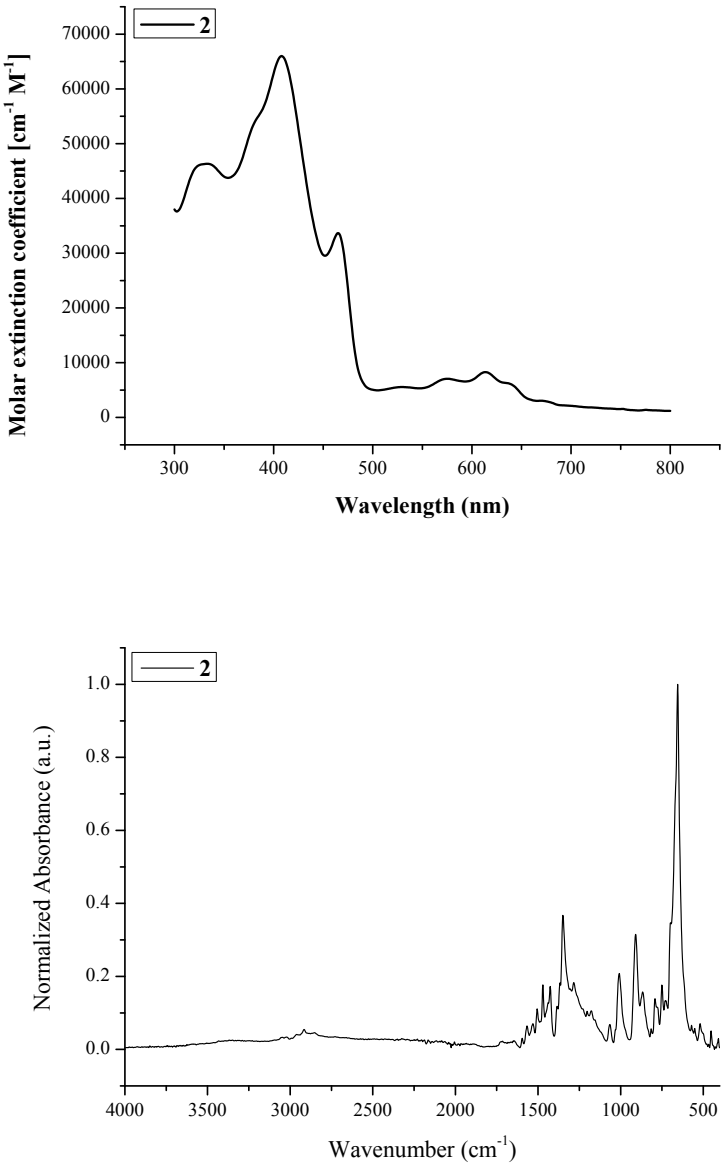

Figure S7. Molar absorptivity (in dichloromethane) and solid state ATR-FTIR spectra of **2**.

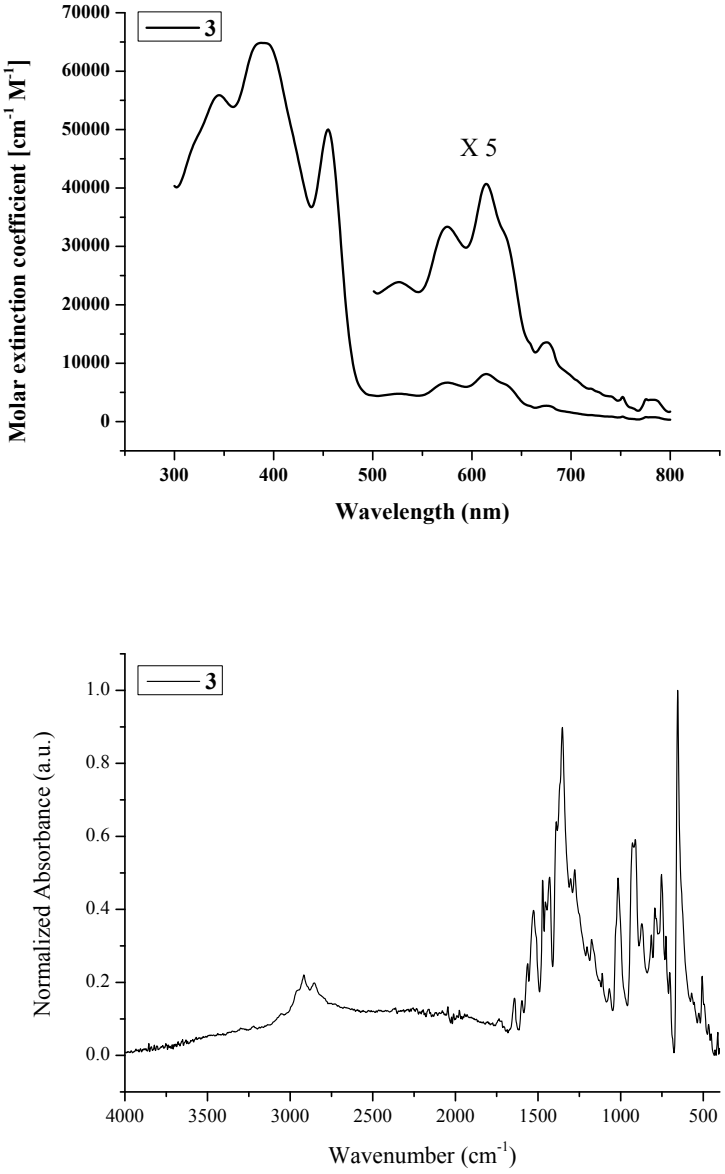

Figure S8. Molar absorptivity (in dichloromethane) and solid state ATR-FTIR spectra of **3**.

HRMS-ESI results of **1-3** including simulated patterns for $[M]^+$ and $[M+H]^+$.

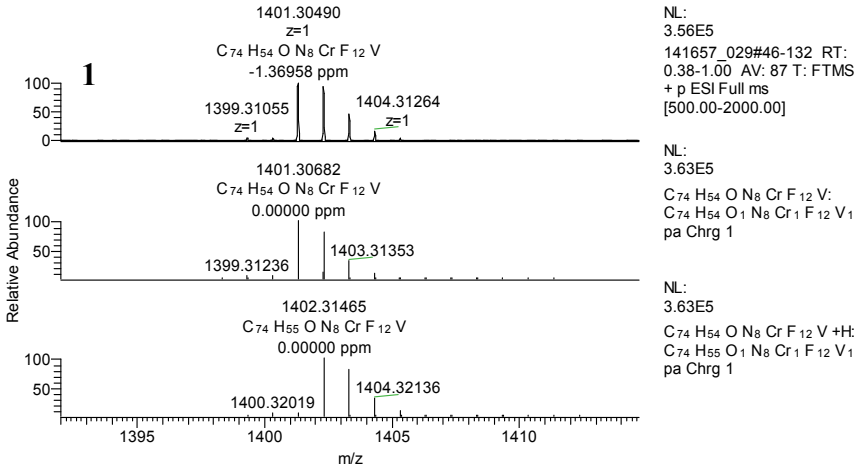

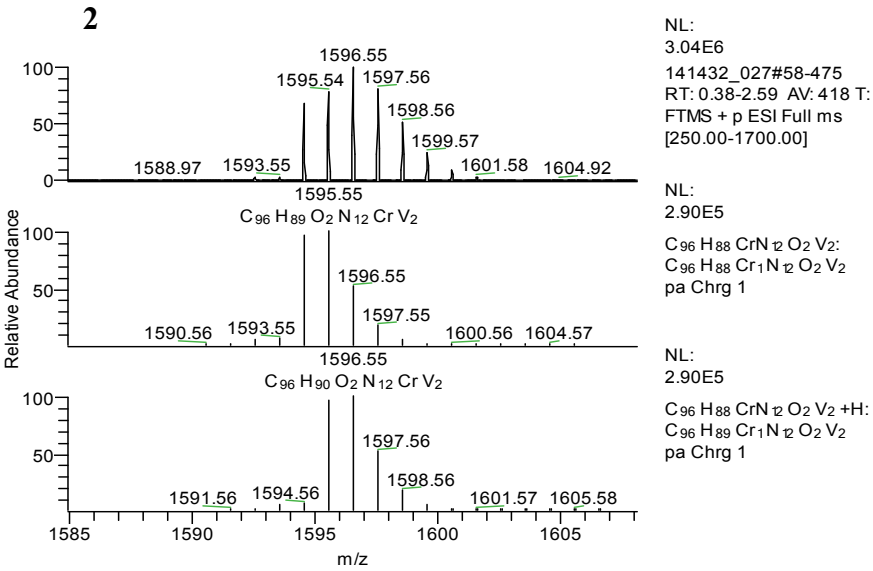

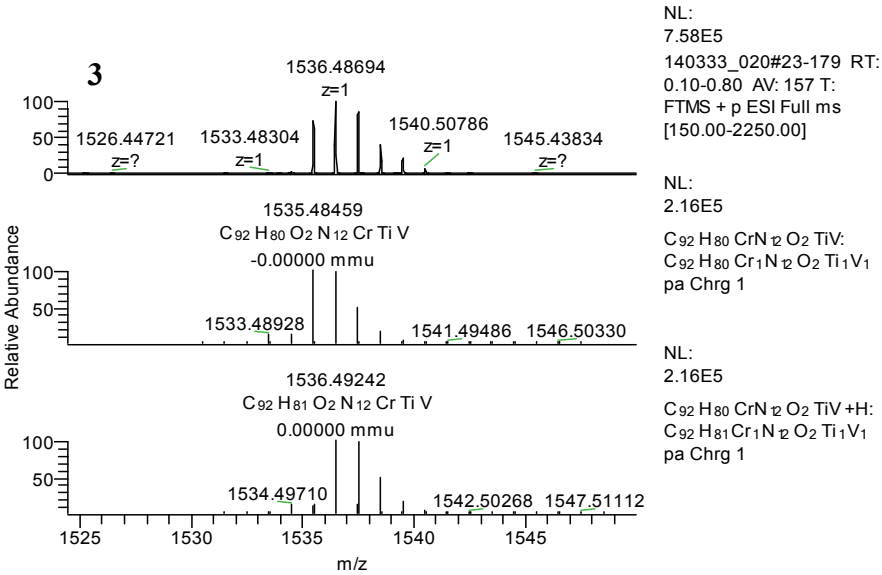

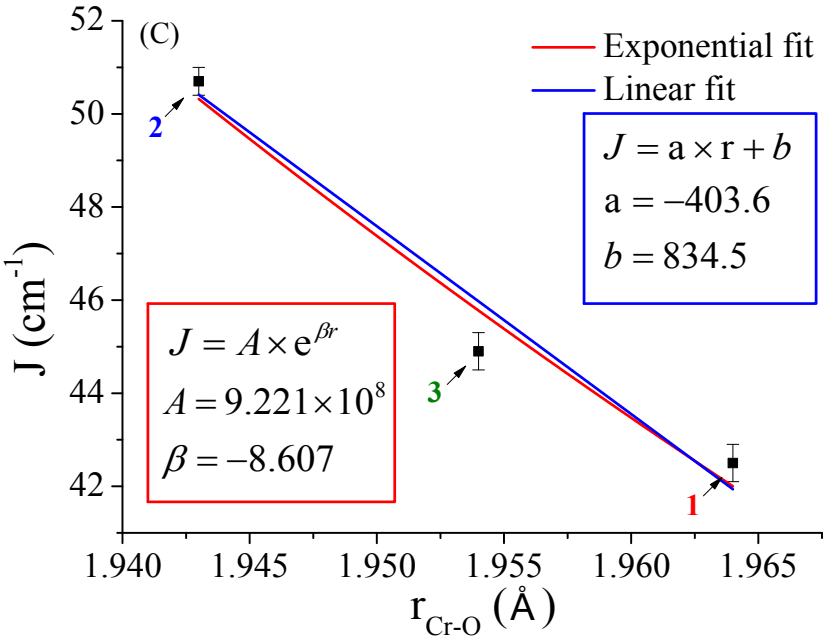

Figure S9. Exchange coupling J versus Cr−O bond distance for **1-3**. Linear fit is performed as comparison to exponential fit which illustrates that a = 834.5 and b = -403.6 Å for equation of J =a*r+b

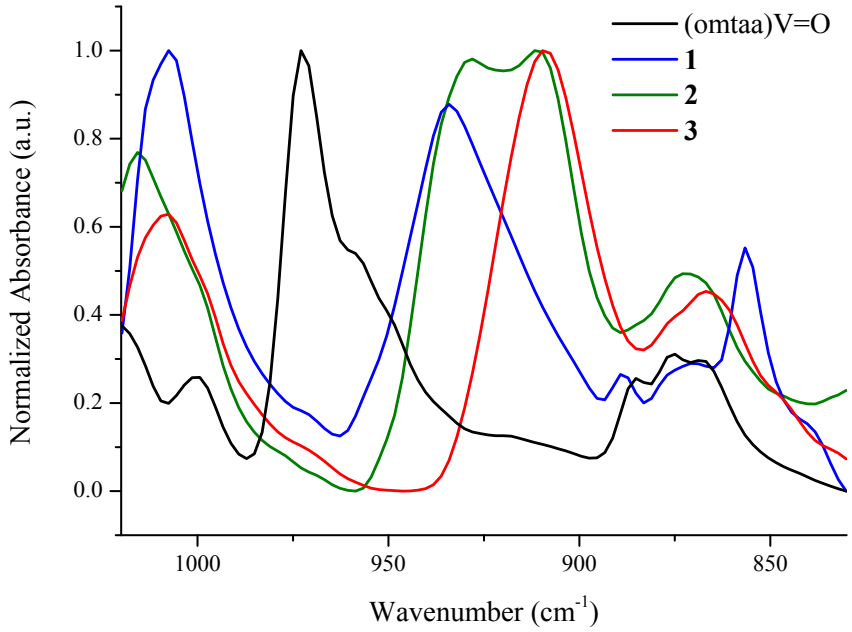

Figure S10. Overlay of ATR-FTIR spectra of (omtaa)V=O and **1-3**.

Additional Table

Table S1. Crystal data and structure refinement details for **1-3**

Identification	(omtaa)V═O	**1**	**2**	**3**
Ccdc number	1049244	1049246	1049245	1049247
Empirical formula	$C_{27}H_{32}Cl_2N_4OV$	$C_{80}H_{66}Cl_{13}CrF_{12}N_8OV$	$C_{100}H_{96}Cl_8CrF_6N_{12}O_2SbV_2$	$C_{92}H_{80}CrF_6N_{12}O_2SbTiV$
Formula weight	550.4	1947.19	2171.11	1772.27
Temperature/K	110	110.1	100.07	110.1
Crystal system	triclinic	triclinic	monoclinic	Monoclinic
Space group	P-1	P-1	$P2_1/c$	$P2_1/c$
a/Å	8.5779(7)	13.1820(5)	19.3129(7)	18.4365(8)
b/Å	12.0788(10)	13.6961(6)	22.2548(7)	22.6229(10)
c/Å	12.8219(11)	27.0875(11)	24.0941(9)	24.1293(10)
α/°	79.362(4)	101.953(2)	90	90
β/°	78.253(4)	95.065(2)	107.631(2)	108.861(2)
γ/°	79.424(4)	108.123(2)	90	90
Volume/Å^3	1263.52(18)	4485.3(3)	9869.3(6)	9523.6(7)
Z	2	2	4	4
ρ_{calc}g/cm^3	1.447	1.442	1.461	1.236
μ/mm^{-1}	0.633	0.685	0.845	0.629
F(000)	574	1972	4428	3624
Crystal size/mm^3	0.575 × 0.32 × 0.212	0.568 × 0.391 × 0.274	0.716 × 0.598 × 0.294	0.506 × 0.465 × 0.12
Radiation	MoKα (λ = 0.71073)	MoKα (λ = 0.71073)	MoKα (λ = 0.71073)	MoKα (λ = 0.71073)
2Θ range for data collection/°	3.47 to 65.154	1.558 to 52.746	2.212 to 51.36	2.948 to 50.054
Index ranges	-12 ≤ h ≤ 12, -18 ≤ k ≤ 17, -19 ≤ l ≤ 17	-16 ≤ h ≤ 16, -17 ≤ k ≤ 17, -33 ≤ l ≤ 33	-18 ≤ h ≤ 23, -27 ≤ k ≤ 27, -29 ≤ l ≤ 29	-21 ≤ h ≤ 21, -26 ≤ k ≤ 26, -28 ≤ l ≤ 28
Reflections collected	43863	102867	108776	203167
Independent reflections	9191 [R_{int} = 0.0205, R_{sigma} = 0.0147]	18323 [R_{int} = 0.0428, R_{sigma} = 0.0387]	18697 [R_{int} = 0.0837, R_{sigma} = 0.0466]	16810 [R_{int} = 0.0409, R_{sigma} = 0.0229]
Data/restraints/parameters	9191/0/343	18323/0/1092	18697/1/1251	16810/11/1109
Goodness-of-fit on F^2	1.057	1.044	1.081	1.15
Final R indexes [I>=2σ (I)]	R_1 = 0.0330, wR_2 = 0.0959	R_1 = 0.0556, wR_2 = 0.1421	R_1 = 0.0826, wR_2 = 0.1926	R_1 = 0.0774, wR_2 = 0.1933
Final R indexes [all data]	R_1 = 0.0355, wR_2 = 0.0981	R_1 = 0.0840, wR_2 = 0.1655	R_1 = 0.1166, wR_2 = 0.2282	R_1 = 0.1012, wR_2 = 0.2122
Largest diff. peak/hole / e Å^{-3}	0.58/-0.81	0.96/-1.00	1.19/-1.60	0.82/-1.01

References

(1) Liston, D. J.; West, B. O. *Inorg. Chem.* **1985**, *24*, 1568.

(2) Huang, T.; Wu, X.; Weare, W. W.; Sommer, R. D. *Eur. J. Inorg. Chem.* **2014**, *2014*, 5662.

(3) Yang, C.-H.; Ladd, J. A.; Goedken, V. L. *J. Coord. Chem.* **1988**, *19*, 235.

(4) Yang, C.-H.; Ladd, J. A.; Goedken, V. L. *J. Coord. Chem.* **1988**, *18*, 317.

(5) Buchler, J.; Kokisch, W.; Smith, P. In *Novel Aspects Structure and Bonding*; Springer Berlin Heidelberg: 1978; Vol. 34, p 79.

(6) Coe, B. J.; Glenwright, S. J. *Coord. Chem. Rev.* **2000**, *203*, 5.

(7) Poulton, J. T.; Folting, K.; Streib, W. E.; Caulton, K. G. *Inorg. Chem.* **1992**, *31*, 3190.